

5.1 Introduction

This chapter¹ describes the adding-doubling method for solving the radiative transport equation. The advantages and disadvantages of the method are presented, followed by sections describing its theory and computer implementation. A detailed example is given with intermediate numerical results. Accurate tables with values of reflection and transmission for slabs of varying thicknesses with mismatched boundaries are given.

5.1.1 Goal

The goal is to develop a model that generates fast and accurate estimates of light distributions in any biological tissue. Such a model should generate internal fluence rates as well as the amount of light reflected or transmitted. An accurate model could serve as a “gold standard” for evaluating less accurate models (e.g., Kubelka-Munk, diffusion), and to verify Monte Carlo implementations. Finally, a fast and accurate model could serve as the cornerstone of a technique to derive intrinsic optical properties from measurements of reflection and transmission [1, 2].

Since this fast and accurate model is intended for light propagation in biological tissues, the particular features associated with this medium must be incorporated:

- There should be no restriction on the ratio of scattering to absorption, since the ratio varies from nearly zero in the both the ultraviolet ($\lesssim 300$ nm due to protein absorption) and the mid-infrared ($\gtrsim 1300$ nm due to water absorption) to large values in the therapeutic window in the red and near-infrared [3, 4].
- There should be no restrictions on the scattering anisotropy, since tissue scattering tends to be strongly forward-peaked (0.7-0.99) [4, 5].
- Internal reflection at boundaries should be included, since air-tissue interfaces are common.

If we neglect any wave phenomena associated with light (e.g., diffraction, interference), then modeling light propagation in tissue is essentially equivalent to solving the full time-dependent radiative transport equation [6, 7]. Analytic solutions to this general equation are not available and the only accurate numerical solutions are based on slow Monte Carlo techniques [8, 9].

5.1.2 Assumptions

The following assumptions make the radiative transport equation more tractable

- no time dependence,
- a geometry consisting of uniform layers of finite thickness and infinite extent in directions parallel to the surface,
- tissue layers with uniform scattering and absorbing properties, and
- uniform illumination by collimated or diffuse light.

In general these assumptions restrict the type and shape of the tissue sample, but do not contradict the known light propagation behavior of tissue. A model that only makes these assumptions will retain relevance to many tissue optics problems. If these assumptions are not valid, say when beam spreading from a finite source is important, then the fluence rates can be accurately calculated using the Monte Carlo method [10].

¹S. A. Prahl, “The Adding-Doubling Method,” in *Optical Thermal Response of Laser Irradiated Tissue*, edited by A. J. Welch and M. J. C. van Gemert, Plenum Press, New York, pp. 101–129, 1995

5.1.3 Why Adding-Doubling?

Since the light propagation model must accurately simulate samples with arbitrary scattering to absorption ratios, anisotropic scattering and boundaries, no analytical and few numerical options exist. Common approximations like the diffusion equation [11], random walk models [12], Kubelka-Munk [13], the seven-flux model [14], and Chandrasekhar's X and Y functions [15] place restrictions on one or more of the basic tissue properties. Two methods, discrete ordinates [16] and adding-doubling [17], allow accurate solution of the radiative transport equation for anisotropic scattering and mismatched boundaries. Adding-doubling works naturally with layered media and yields reflection and transmission readily, while discrete ordinates generates internal fluences easily. We select the adding-doubling method because reflectance is important for diagnostic applications using light. Furthermore when measuring the optical properties of a sample, the only values needed are the total reflection and transmission of the sample [1].

5.1.4 General Description

The doubling method assumes knowledge of the reflection and transmission properties for a single thin homogeneous layer. The reflection and transmission of a slab twice as thick is found by juxtaposing two identical slabs and summing the contributions from each slab [17, 18]. The reflection and transmission for an arbitrarily thick slab are obtained by repeatedly doubling until the desired thickness is reached. The adding method extends the doubling method to dissimilar slabs, thereby allowing one to simulate media with different layers and/or internal reflection at boundaries.

The doubling method was introduced by van de Hulst for solving the radiative transport equation in a slab geometry [19]. The advantages of the adding-doubling method are that only integrations over angle are required, physical interpretation of results can be made at each step, the method is equivalent for isotropic and anisotropic scattering, and results are obtained for all angles of incidence used in the integration [20]. The disadvantages are that it is (a) awkward to calculate internal fluences, (b) restricted to layered geometries with uniform irradiation, and (c) necessary that each layer have homogeneous optical properties. In practice, internal fluences are often not needed so (a) is not a problem. When fluences are needed at a particular depth, they can be calculated by finding the reflection and transmission matrices for light propagation through the material above that depth as well as the matrices for everything below. These matrices are used in (5.24) and (5.25) to find the upward and downward radiance at the interface between these layers. The fluence follows directly once the radiance as a function of angle is known. Items (b) and (c) place restrictions on the sample geometry — the samples must have homogeneous layers and be uniformly illuminated (e.g., finite beam irradiance is not allowed nor any situation causing variation in the light field perpendicular to the direction of propagation.) The adding-doubling method is well-suited to iterative problems because it provides accurate total reflection and transmission calculations with relatively few integration points. The method is very fast for small numbers of integration points, and consequently iteration is practical.

This chapter describes an implementation of the adding-doubling method for solving the radiative transport equations numerically. Any phase function may be chosen to characterize scattering in the medium and any tissue optical thickness is possible. The method is accurate for any ratio of scattering to absorption. Tissue layers with different optical properties may be added together to find the reflection and transmission for inhomogeneous layered media. Light incident on a slab must be azimuthally independent. Boundaries may have varied effects, but only those characterized by specular Fresnel reflection are discussed.

In this chapter, the details of implementation are gathered from a range of sources so that the reader may implement the adding-doubling method. The basic equations have been outlined by Plass *et al.* are repeated here for completeness [18]. One especially tricky area is in the implementation of boundary conditions for mismatched boundaries [1] and this aspect is treated in detail.

5.2 Theory

The following assumptions are made throughout this chapter: the distribution of light is independent of time, samples have homogeneous optical properties, the sample geometry is an infinite plane-parallel slab of finite thickness, the tissue has a uniform index of refraction, internal reflection at boundaries is governed by Fresnel's law, and the light is

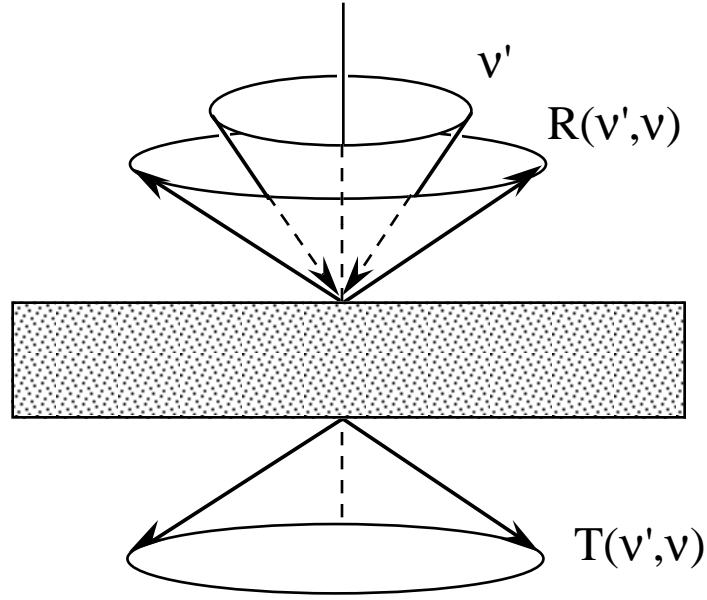


Figure 1: Light incident at an angle ν' that is reflected and transmitted by a slab at an angle ν .

unpolarized. A non-absorbing layer with a different index of refraction may be present at the boundaries (glass slide). Finally, the slab is assumed to have no internal sources.

This section has four parts. The first describes the nomenclature and geometries used. The second explicitly gives the relationship between reflection function $R(\nu', \nu)$ and the reflection matrix \mathbf{R}_{ij} . The third introduces quadrature as an integration method. The fourth gives the matrix formulas for combining two dissimilar layers.

5.2.1 Notation

Since the entire discussion that follows assumes azimuthal symmetry, the behavior of a light ray is determined by the angle it makes with the normal. We use the notation $\nu = \cos \theta$ to specify direction. If the absorption and single scattering coefficients are denoted by μ_a and μ_s , then the albedo is defined as $a = \mu_s / (\mu_s + \mu_a)$. The single scattering phase function $p(\nu)$ is the fraction of light scattered in direction ν from the incident direction. The phase function is normalized so that

$$\int_{4\pi} p(\nu) d\omega = 2\pi \int_{-1}^1 p(\nu) d\nu \equiv 1 \quad (5.1)$$

The scattering anisotropy g is defined as the average cosine of the phase function over all angles,

$$g \equiv 2\pi \int_{-1}^1 p(\nu) \nu d\nu \quad (5.2)$$

The dimensionless optical distance τ is defined as $\tau = (\mu_a + \mu_s)d$, where d is the physical distance within the medium.

A cone of light incident at an angle ν on an arbitrary turbid slab will backscatter (reflect) and transmit different amounts of light depending on the angle of departure. We will follow the definition of van de Hulst [17] for the reflection $R(\nu', \nu)$ and transmission $T(\nu', \nu)$ functions. The reflection function $R(\nu', \nu)$ is defined as the radiance reflected by the slab in direction ν for light conically incident from the ν' direction (Figure 1). The reflection is normalized to an incident diffuse flux π , This definition has the advantage that $R(\nu', \nu)$ has finite non-zero values when $\nu = 0$ or $\nu' = 0$ and thereby improves the computational accuracy. Furthermore, $R(\nu', \nu)$ is the ratio of the

actual reflection function to the reflection function of an ideal white Lambertian surface. The transmission function is defined similarly.

With this definition of the reflection function, the reflected intensity distribution I_{ref} for an azimuth-independent incident intensity I_{in} is

$$I_{\text{ref}}(\nu) = \int_0^1 I_{\text{in}}(\nu') R(\nu', \nu) 2\nu' d\nu' \quad (5.3)$$

Both I_{in} and I_{ref} have units of power per unit solid angle. To obtain the total reflection for normal irradiance R_c

$$\begin{aligned} R_c &= \int_0^1 \int_0^1 R(\nu', \nu) \frac{\delta(1-\nu')}{2\nu'} 2\nu' d\nu' 2\nu d\nu \\ &= \int_0^1 R(1, \nu) 2\nu d\nu \end{aligned} \quad (5.4)$$

The total transmission for collimated irradiance T_c is

$$T_c = \int_0^1 T(1, \nu) 2\nu d\nu \quad (5.5)$$

The total reflection R_d and total transmission T_d for diffuse irradiance are

$$R_d = \int_0^1 \int_0^1 R(\nu', \nu) 2\nu' d\nu' 2\nu d\nu \quad (5.6)$$

and

$$T_d = \int_0^1 \int_0^1 T(\nu', \nu) 2\nu' d\nu' 2\nu d\nu \quad (5.7)$$

5.2.2 Matrix Approximation

Consider a homogeneous slab with isotropic scattering ($g = 0.0$), a fixed albedo ($a = 0.9$), optical thickness ($\tau = 1$), and matched boundaries. For an infinitely wide beam of light normally incident on this slab the reflection will vary with the exit angle (Figure 2). The reflection curve can be approximated by the four circles shown in Figure 2. If more points are used then the approximation will be better. The number of points will be denoted by M , and $M = 4$ gives a very fast, reasonably accurate estimate. Four approximation points are used in the sample calculations. (The more accurate results tabulated at the end of this chapter use $M = 32$.)

The four angles used to approximate the transmission are chosen according to the quadrature scheme used (see the next subsection). The angles shown in Figure 2 are

$$\begin{bmatrix} \nu_1 \\ \nu_2 \\ \nu_3 \\ \nu_4 \end{bmatrix} = \begin{bmatrix} 0.09 \\ 0.41 \\ 0.79 \\ 1.00 \end{bmatrix} = \begin{bmatrix} \sim 85^\circ \\ \sim 66^\circ \\ \sim 38^\circ \\ 0^\circ \end{bmatrix} \quad (5.8)$$

The corresponding reflection values are

$$\begin{bmatrix} R(\nu_4, \nu_1) \\ R(\nu_4, \nu_2) \\ R(\nu_4, \nu_3) \\ R(\nu_4, \nu_4) \end{bmatrix} = \begin{bmatrix} 0.37 \\ 0.32 \\ 0.24 \\ 0.21 \end{bmatrix} \quad (5.9)$$

Similar vectors for reflection exist for the other three angles of incidence ν_1 , ν_2 , and ν_3 . By combining these into a single matrix yields the reflection matrix for this particular slab,

$$\mathbf{R} = \begin{bmatrix} 1.66 & 0.72 & 0.45 & 0.37 \\ 0.72 & 0.52 & 0.37 & 0.32 \\ 0.45 & 0.37 & 0.28 & 0.24 \\ 0.37 & 0.32 & 0.24 & 0.21 \end{bmatrix} \quad (5.10)$$

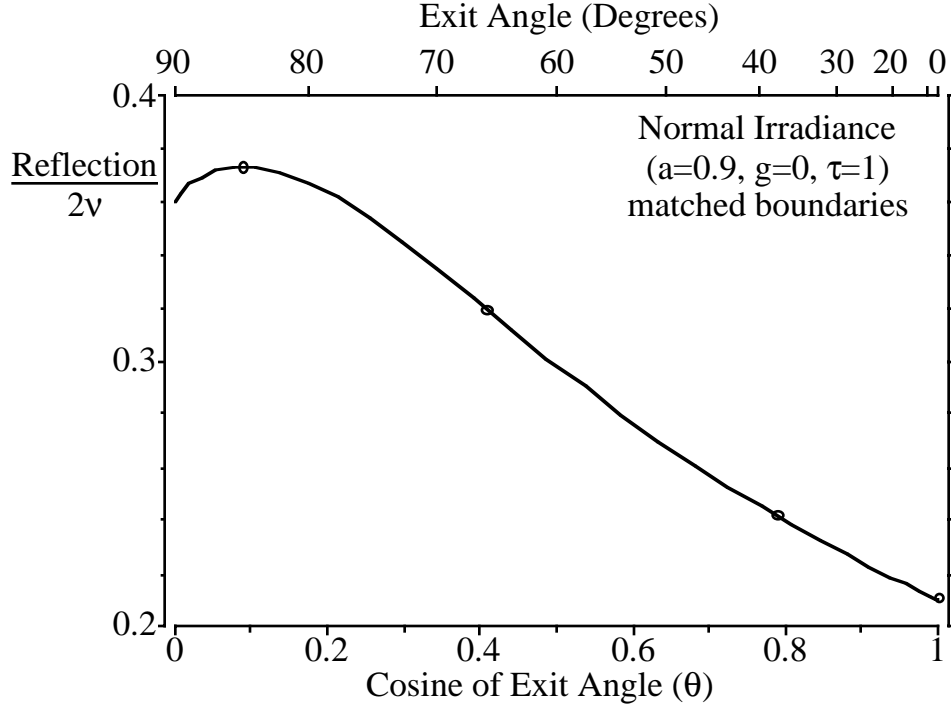


Figure 2: Reflection from a normally irradiated slab with isotropic scattering, an optical thickness of unity and an albedo equal to 0.9. The four circles represent quadrature points.

Note that this reflection matrix is symmetric: $R(\nu_i, \nu_j) = R(\nu_j, \nu_i)$. The individual entries in the reflection matrix can be greater than unity because each entry is divided by twice its quadrature angle.

5.2.3 Quadrature

Since the adding-doubling method consists of integrating various combinations of reflection and transmission functions, the integration method is crucial. For example, the total reflection for normal collimated irradiance is given by

$$R_c = \int_0^1 R(1, \nu) 2\nu d\nu \quad (5.11)$$

This integral may be approximated using quadrature. For example, consider the integration of a function $f(x)$ over the interval (a, b) with a weighting function $g(x)$ using M points

$$\int_a^b f(x)g(x) dx \approx \sum_{i=1}^M f(x_i)w_i \quad (5.12)$$

The integration points x_i and weights w_i are chosen in such a way that the integration will integrate a polynomial of degree $2M$ (or possibly $2M - 2$ depending on the method) exactly. The approximation for R_c is

$$\int_0^1 R(1, \nu) 2\nu d\nu \approx \sum_{i=1}^M 2\nu_i w_i \mathbf{R}_{iM} \quad (5.13)$$

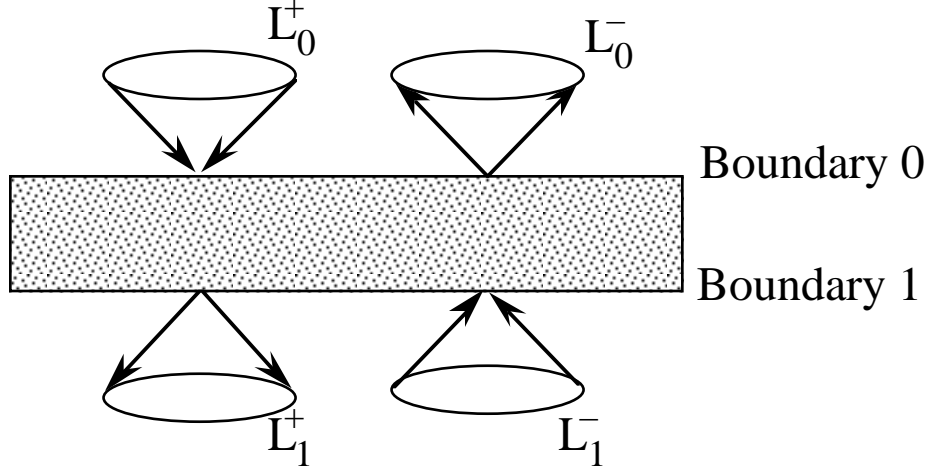


Figure 3: Nomenclature for the derivation of the adding-doubling equations. A minus sign indicates upward travelling light and a plus sign downward directed light.

The extension to two arbitrary functions is

$$\int_0^1 A(v, v') B(v', v'') 2v' dv' \approx \sum_{j=1}^M \mathbf{A}_{ij} 2v_j w_j \mathbf{B}_{jk} \quad (5.14)$$

This explicitly shows the relation between integration and matrix multiplication: the only difference being the factor of $2v_j w_j$ that must be included,

$$\mathbf{A} \mathbf{B} \equiv \sum_{j=1}^M \mathbf{A}_{ij} 2v_j w_j \mathbf{B}_{jk} \approx \int_0^1 A(v, v') B(v', v'') 2v' dv' \quad (5.15)$$

The identity matrix \mathbf{E} for matrix multiplication of this type is

$$\mathbf{E}_{ij} = \frac{1}{2v_i w_i} \delta_{ij} \quad (5.16)$$

Here δ_{ij} is the Kronecker delta. Grant and Hunt have shown that an algebra based on this implied multiplication is a semi-group [21, 22], and have proven that all manipulations that follow are valid.

5.2.4 Matrix Relations for Adding Layers

This derivation follows Plass *et al.* [18] with the terms representing internal light sources omitted for clarity. Define \mathbf{T}^{nm} and \mathbf{R}^{nm} as the transmission and reflection operators for light incident on side n and moving towards side m of a slab. Homogeneous tissues have no preferred direction and so $\mathbf{T}^{nm} = \mathbf{T}^{mn}$ and $\mathbf{R}^{nm} = \mathbf{R}^{mn}$. As in Figure 3, let the vector $\mathbf{L}^{0+}(v)$ denote the radiance incident from on side 0 in a downward direction (indicated by the +). Let $\mathbf{L}^{1-}(v)$ denote the radiance incident on side 1 in an upward direction (indicated by the -). Similarly define \mathbf{L}^{0-} and \mathbf{L}^{1+} as the radiance exiting from sides 0 and 1 respectively.

The downward radiance from side 1 is the sum of the transmitted incident radiance from side 0 and the reflected radiance from side 1,

$$\mathbf{L}^{1+} = \mathbf{T}^{01} \mathbf{L}^{0+} + \mathbf{R}^{10} \mathbf{L}^{1-} \quad (5.17)$$

The upward radiance from side 0 is the transmitted radiance from side 1 and the reflected radiance from side 0

$$\mathbf{L}^{0-} = \mathbf{R}^{01} \mathbf{L}^{0+} + \mathbf{T}^{10} \mathbf{L}^{1-} \quad (5.18)$$

Analogous formulas apply to a layer with sides 1 and 2

$$\mathbf{L}^{2+} = \mathbf{T}^{12}\mathbf{L}^{1+} + \mathbf{R}^{21}\mathbf{L}^{2-} \quad (5.19)$$

$$\mathbf{L}^{1-} = \mathbf{R}^{12}\mathbf{L}^{1+} + \mathbf{T}^{21}\mathbf{L}^{2-} \quad (5.20)$$

Juxtaposition of layers (01) and (12) yields a combined layer (02). The equations for the layer with sides 0 and 2 are

$$\mathbf{L}^{2+} = \mathbf{T}^{02}\mathbf{L}^{0+} + \mathbf{R}^{20}\mathbf{L}^{2-} \quad (5.21)$$

$$\mathbf{L}^{0-} = \mathbf{R}^{02}\mathbf{L}^{0+} + \mathbf{T}^{20}\mathbf{L}^{2-} \quad (5.22)$$

Presumably, the reflection and transmission operators for the (01) and (12) layers are known. To express reflection and transmission operators for the (02) layer in terms of the individual layers we left multiply Equation (5.17) by \mathbf{R}^{12} and add it to Equation (5.20) to get

$$(\mathbf{E} - \mathbf{R}^{12}\mathbf{R}^{10})\mathbf{L}^{1-} = \mathbf{R}^{12}\mathbf{T}^{01}\mathbf{L}^{0+} + \mathbf{T}^{21}\mathbf{L}^{2-} \quad (5.23)$$

Solving for \mathbf{L}^{1-} yields

$$\mathbf{L}^{1-} = (\mathbf{E} - \mathbf{R}^{12}\mathbf{R}^{10})^{-1}(\mathbf{R}^{12}\mathbf{T}^{01}\mathbf{L}^{0+} + \mathbf{T}^{21}\mathbf{L}^{2-}) \quad (5.24)$$

This equation expresses the upward radiance at the interface between two layers. An equation for the downward mid-layer radiance can be obtained by left multiplying Equation (5.20) by \mathbf{R}^{12} and adding it to Equation (5.17)

$$\mathbf{L}^{1+} = (\mathbf{E} - \mathbf{R}^{10}\mathbf{R}^{12})^{-1}(\mathbf{T}^{01}\mathbf{L}^{0+} + \mathbf{R}^{10}\mathbf{T}^{21}\mathbf{L}^{2-}) \quad (5.25)$$

Substituting Equation (5.25) into Equation (5.19) yields

$$\begin{aligned} \mathbf{L}^{2+} &= \left[\mathbf{T}^{12}(\mathbf{E} - \mathbf{R}^{10}\mathbf{R}^{12})^{-1}\mathbf{T}^{01} \right] \mathbf{L}^{0+} \\ &+ \left[\mathbf{T}^{12}(\mathbf{E} - \mathbf{R}^{10}\mathbf{R}^{12})^{-1}\mathbf{R}^{10}\mathbf{T}^{21} + \mathbf{R}^{21} \right] \mathbf{L}^{2-} \end{aligned} \quad (5.26)$$

Comparing this with Equation (5.21) indicates

$$\mathbf{T}^{02} = \mathbf{T}^{12}(\mathbf{E} - \mathbf{R}^{10}\mathbf{R}^{12})^{-1}\mathbf{T}^{01} \quad (5.27)$$

$$\mathbf{R}^{20} = \mathbf{T}^{12}(\mathbf{E} - \mathbf{R}^{10}\mathbf{R}^{12})^{-1}\mathbf{R}^{10}\mathbf{T}^{21} + \mathbf{R}^{21} \quad (5.28)$$

Similarly Equation (5.24) can be substituted into Equation (5.18) and compared to Equation (5.22) to obtain

$$\mathbf{T}^{20} = \mathbf{T}^{10}(\mathbf{E} - \mathbf{R}^{12}\mathbf{R}^{10})^{-1}\mathbf{T}^{21} \quad (5.29)$$

$$\mathbf{R}^{02} = \mathbf{T}^{10}(\mathbf{E} - \mathbf{R}^{12}\mathbf{R}^{10})^{-1}\mathbf{R}^{12}\mathbf{T}^{01} + \mathbf{R}^{01} \quad (5.30)$$

Equations (5.27)–(5.30) define the reflection and transmission operators for a combined layer in terms of the operators for each individual layer. Repeatedly using these equations allows the reflection and transmission of an arbitrary layered sample. If the internal radiance required, then the sample is divided into two pieces at the depth at which the radiance is wanted. After calculating the reflection and transmission properties of both pieces, the internal radiance is found using Equations (5.24) and (5.25).

The equations given above are entirely appropriate if the direct beam coincides with one of the quadrature angles. If this is not true, then the equations for doubling become more complex. Equations with separate terms for primary and scattered light are given in Hansen and Travis [23] and van de Hulst [17].

5.3 Implementation

The implementation of the the adding-doubling method for calculating the reflection and transmission of a turbid slab in a medium with a different index of refraction consists of the following steps

- Choose quadrature scheme [1]
- Generate starting layer [24]
- Generate boundary layers [25]
- Double starting layer until desired thickness is reached [17]
- Add boundary layers to this [18]
- Calculate reflection and transmission [18]

5.3.1 Quadrature

Nearly every integration in the adding-doubling method is over the range zero to one. Three quadrature methods which naturally span this range and have the desired weighting function are Gaussian, Lobatto, and Radau [15,26,27]. These methods have nearly equal accuracy [18], but vary in whether or not the endpoints of integration are included as quadrature points. The specific choice of quadrature methods is determined by the boundary conditions. In Gaussian quadrature, neither endpoint (0 or 1) is included. In Lobatto quadrature both endpoints are included. In Radau quadrature, one quadrature point may be specified and neither endpoint need be included. To avoid extrapolation/interpolation errors, the $\nu = 1$ endpoint (normal incidence) is usually chosen as a quadrature angle.

Internal reflection at the boundaries (due to mismatched indices of refraction) is included in the calculation by adding an additional layer for each mismatched boundary. The reflection and transmission of this layer is one and zero, respectively, for light incident at angles greater than the critical angle. This changes the effective range of integration. If the cosine of the critical angle is denoted by ν_c for a boundary layer with total internal reflection, then the effective range of integration is reduced down to ν_c to 1 (because the rest of the integration range is now zero). To maintain integration accuracy, the integral is broken into two parts and each is evaluated using quadrature over the specified subrange,

$$\begin{aligned}
 & \int_0^1 A(\nu, \nu') B(\nu', \nu'') 2\nu' d\nu' \\
 = & \int_0^{\nu_c} A(\nu, \nu') B(\nu', \nu'') 2\nu' d\nu' \\
 + & \int_{\nu_c}^1 A(\nu, \nu') B(\nu', \nu'') 2\nu' d\nu'. \tag{5.31}
 \end{aligned}$$

Here $A(\nu, \nu')$ and $B(\nu, \nu')$ represent reflection or transmission functions, and clearly if either is identically zero for values of ν less than ν_c , the integration range is reduced. The calculations in this paper used Gaussian quadrature [28] for the range from 0 to ν_c , thereby avoiding calculations at both endpoints (in particular, the angle $\nu = 0$ is avoided, which may cause division by zero). Radau quadrature is used for the range from ν_c to 1, so $\nu = 1$ could be specified as a quadrature point [27]. Each part of the integration range gets half of the quadrature points; when no critical angle exists, Radau quadrature is used over the entire range.

Radau quadrature requires finding the n roots of the following equation [27].

$$P_{n-1}(x_i) + \frac{x_i - 1}{n} P'_{n-1}(x_i) = 0 \tag{5.32}$$

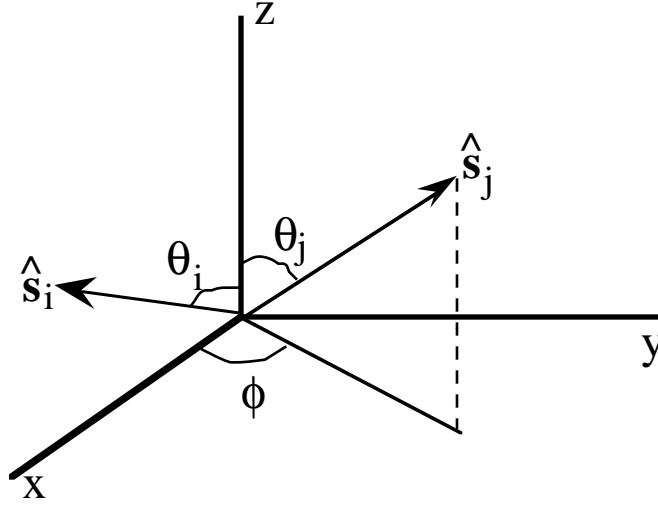


Figure 4: Nomenclature for derivation of subtended angle.

Here $P_n(x)$ is the n th Legendre polynomial of order zero and $P'_{n-1}(x_i)$ is the first derivative of the $n - 1$ Legendre polynomial. These roots are the required quadrature points for the integration range -1 to 1. To modify for the range v_c to 1 the following relations are needed to find the necessary integration angles v_i and weights w_i

$$\begin{aligned} v_i &= \frac{1 + v_c - (1 - v_c)x_i}{2} \\ w_i &= \frac{1 - v_c}{(1 - x_i)\sqrt{P'_{n-1}(x_i)}} \end{aligned} \quad (5.33)$$

The n th integration angle v_n corresponds with $x_n = -1$ (normal incidence).

The n integration points for Gaussian quadrature for the interval -1 to 1 are the roots of

$$P_n(x_i) = 0 \quad (5.34)$$

The required adjustment for the integration range 0 to v_c is

$$v_i = \frac{v_c}{2}(1 - x_i) \quad \text{and} \quad w_i = \frac{2v_c}{(1 - x_i^2)[P'_n(x_i)]^2} \quad (5.35)$$

An algorithm which takes advantage of the many properties of orthogonal polynomials to find all the roots of a particular Legendre polynomial is given by Press *et al.* [28].

5.3.2 The Redistribution Function

The single scattering phase function $p(\nu)$ for a tissue determines the amount of light scattered at an angle $\nu = \cos \theta$ from the direction of incidence. The dot product of the unit vectors \hat{s}_i and \hat{s}_j associated with the incident and scattered light directions

$$\hat{s}_i \cdot \hat{s}_j = |\hat{s}_i| |\hat{s}_j| \cos \theta = \nu \quad (5.36)$$

can be used to relate ν to the angles v_i and v_j (see Figure 4). If the inward normal to the slab is parallel to the z -axis and \hat{s}_i lies in the xz -plane, then $\hat{s}_i = (\sin \theta_i, 0, \cos \theta_i) = (\sqrt{1 - v_i^2}, 0, v_i)$. If ϕ is the azimuthal angle

from the positive x -axis to the projection of $\hat{\mathbf{s}}_j$ onto the xy -plane, then $\hat{\mathbf{s}}_j = (\sin \theta_j \cos \phi, \sin \theta_j \sin \phi, \cos \theta_j) = (\sqrt{1 - v_j^2} \cos \phi, \sqrt{1 - v_j^2} \sin \phi, v_j)$. The subtended angle v is then given by the dot product

$$v = v_i v_j + \sqrt{1 - v_i^2} \sqrt{1 - v_j^2} \cos \phi \quad (5.37)$$

The redistribution function \mathbf{h}_{ij} determines the fraction of light scattered from an incidence cone with angle v_i into a cone with angle v_j . The redistribution function is calculated by averaging the phase function over all possible azimuthal angles for fixed angles v_i and v_j ,

$$h(v_i, v_j) = \frac{1}{2\pi} \int_0^{2\pi} p(v_i v_j + \sqrt{1 - v_i^2} \sqrt{1 - v_j^2} \cos \phi) d\phi \quad (5.38)$$

Note that the angles v_i and v_j may also be negative (light travelling in the opposite direction). The full redistribution matrix may be expressed in terms a 2×2 matrix of $M \times M$ matrices

$$\mathbf{h} = \begin{bmatrix} \mathbf{h}^{--} & \mathbf{h}^{-+} \\ \mathbf{h}^{+-} & \mathbf{h}^{++} \end{bmatrix} \quad (5.39)$$

The first plus or minus sign indicates the sign in front of the incident angle and the second is the sign of the direction of the scattered light.

When the cosine of the angle of incidence or exitance is unity ($v_i = 1$ or $v_j = 1$), then the redistribution function $h(1, v_j)$ is equivalent to the phase function $p(v_j)$. In the case of isotropic scattering, the redistribution function is a constant

$$\frac{h(v_i, v_j)}{4\pi} = p(v) = \frac{1}{4\pi}. \quad (5.40)$$

For Henyey-Greenstein scattering, the redistribution function can be expressed in terms of the complete elliptic integral of the second kind $E(x)$ [29]

$$h(v_i, v_j) = \frac{2}{\pi} \frac{1 - g^2}{(\alpha - \gamma)\sqrt{\alpha + \gamma}} E\left(\sqrt{\frac{2\gamma}{\alpha + \gamma}}\right) \quad (5.41)$$

where g is the average cosine of the Henyey-Greenstein phase function and

$$\alpha = 1 + g^2 - 2g v_i v_j \quad \text{and} \quad \gamma = 2g \sqrt{1 - v_i^2} \sqrt{1 - v_j^2} \quad (5.42)$$

The function $E(x)$ may be calculated using algorithms found in Press *et al.* [28].

Other phase functions require numerical integration of Equation (5.38). If the phase function is highly anisotropic, then the integration over the azimuthal angle is particularly difficult and care must be taken to ensure that the integration is accurate. This is important because errors in the redistribution function enter directly into the reflection and transmission matrices for thin layers. Any errors will be doubled with each successive addition of layers and small errors will rapidly increase.

An alternate way to calculate the redistribution function is the δ - M method [30]. This method works especially well for highly anisotropic phase functions. The number of quadrature points is specified by M . The δ - M method approximates the true phase function by a phase function consisting of a Dirac delta function and $M - 1$ Legendre polynomials

$$p^*(v) = 2g^M \delta(1 - v) + (1 - g^M) \sum_{k=0}^{M-1} (2k + 1) \chi_k^* P_k(v) \quad (5.43)$$

where

$$\chi_k^* = \frac{\chi_k - g^M}{1 - g^M} \quad \text{and} \quad \chi_k = \frac{1}{2} \int_0^1 p(v) P_k(v) dv \quad (5.44)$$

When the δ - M method substitutes $p^*(v) \rightarrow p(v)$, then both the albedo and optical thickness must also be changed, $a^* \rightarrow a$ and $\tau^* \rightarrow \tau$. This approximation is analogous to the similarity transformation often used to improve the

diffusion approximation by moving a part (g^M) of the scattered light into the unscattered component [14, 31]. The new optical thickness and albedo are

$$\tau^* = (1 - ag^M)\tau \quad \text{and} \quad a^* = a \frac{1 - g^M}{1 - ag^M} \quad (5.45)$$

This is equivalent transforming the scattering coefficient as $\mu_s^* = \mu_s(1 - g^M)$. The redistribution function can now be written as

$$h^*(v_i, v_j) = \sum_{k=0}^{M-1} (2k+1) \chi_k^* P_k(v_i) P_k(v_j) \quad (5.46)$$

For the special case of a Henyey-Greenstein phase function,

$$\chi_k^* = \frac{g^k - g^M}{1 - g^M}. \quad (5.47)$$

5.3.3 Layer Initialization

Starting the adding-doubling method requires knowledge of the reflection and transmission operators for a thin slab. Several methods exist for obtaining these operators: diamond initialization [24], infinitesimal generator [32], and successive scattering [33]. Wiscombe found successive scattering to be the worst, and that diamond initialization was better than the infinitesimal generator method about two-thirds of the time [34]. The optical thickness of the starting layer $\Delta\tau^*$ varies with the smallest quadrature angle, since the optical thickness should satisfy [34].

$$\Delta\tau^* < v_1 \quad (5.48)$$

This relation between distance and angles is possible since both v and $\Delta\tau^*$ are dimensionless.

The basic idea behind diamond initialization is to rewrite the time-independent, one-dimensional, azimuthally-averaged, radiative transport equation

$$v \frac{\partial L(\tau, v)}{\partial \tau} + L(\tau, v) = \frac{a^*}{2} \int_{-1}^1 h(v, v') L(\tau, v') dv' \quad (5.49)$$

in a discrete form as

$$\begin{aligned} \pm v_i \frac{\partial L(\tau, \pm v_i)}{\partial \tau} + L(\tau, \pm v_i) \\ = \frac{a^*}{2} \sum_{j=1}^M w_j [h(v_i, v_j) L(\tau, \pm v_j) + h(v_i, -v_j) L(\tau, \mp v_j)] \end{aligned} \quad (5.50)$$

When this equation is integrated over a thin layer from τ_0^* to τ_1^* then get

$$\begin{aligned} \pm v_i [L(\tau_1^*, \pm v_i) - L(\tau_0^*, \pm v_i)] + \Delta\tau^* L_{1/2}(\pm v_i) \\ = \frac{a^*}{2} \sum_{j=1}^M w_j \Delta\tau^* [h(v_i, v_j) L_{1/2}(\pm v_j) + h(v_i, -v_j) L_{1/2}(\mp v_j)] \end{aligned} \quad (5.51)$$

where $\Delta\tau^* = \tau_1^* - \tau_0^*$. The integrated radiance $L_{1/2}(v)$ is

$$L_{1/2}(v) \equiv \frac{1}{\Delta\tau^*} \int_{\tau_0^*}^{\tau_1^*} L(\tau, v) d\tau \quad (5.52)$$

Diamond initialization assumes that this integral can be replaced by a simple average of the radiances at the top and bottom of the layer,

$$L_{1/2}(v) = \frac{1}{2} [L(\tau_0^*, v) + L(\tau_1^*, v)] \quad (5.53)$$

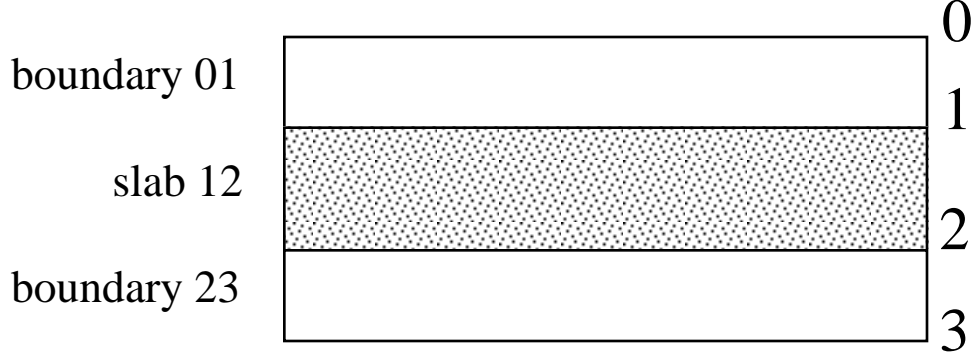


Figure 5: Geometry for calculating light transport through a slab with an index of refraction different from its environment.

After suitable algebraic manipulations [24], Equation (5.52) can be used to express the reflection and transmission of a thin layer with thickness $\Delta\tau^*$ as

$$\mathbf{R}_{\Delta\tau^*} = 2\mathbf{G}\mathbf{B}(\delta_{ij} + \mathbf{A})^{-1} \quad \text{and} \quad \mathbf{T}_{\Delta\tau^*} = 2\mathbf{G} - \delta_{ij} \quad (5.54)$$

where

$$\begin{aligned} \mathbf{A} &= \begin{bmatrix} 1 \\ v_i \end{bmatrix} \delta_{ij} \left(\delta_{ij} - \frac{a^*}{2} \mathbf{h}^{++} \mathbf{c} \right) \frac{\Delta\tau^*}{2} \\ \mathbf{B} &= \frac{a^*}{2} \begin{bmatrix} 1 \\ v_i \end{bmatrix} \delta_{ij} \mathbf{h}^{+-} \mathbf{c} \frac{\Delta\tau^*}{2} \end{aligned} \quad (5.55)$$

and

$$\mathbf{G} = [\delta_{ij} + \mathbf{A} - \mathbf{B}(\delta_{ij} + \mathbf{A})^{-1}\mathbf{B}]^{-1} \quad \text{and} \quad \mathbf{c} = [w_i \delta_{ij}] \quad (5.56)$$

These equations were used to obtain the starting reflection and transmission matrices for all the calculations in this chapter.

5.3.4 Boundary Layers

Boundary conditions are included in the transport calculation by using the adding-doubling equations to add an additional layer that imposes the necessary boundary conditions. The reflection and transmission matrices for this boundary layer depend on the physics of the light interaction at the interface. For example, if we assume that specular reflection is appropriate, then

$$\begin{aligned} \mathbf{R}_{01}(v_i, v_j) &= \frac{r(v_i)}{2v_i} \delta_{ij} \\ \mathbf{T}_{01}(v_i, v_j) &= \frac{1 - r(v_i)}{2v_i} \left(\frac{n_{12}}{n_{01}} \right)^2 \delta_{ij} \end{aligned} \quad (5.57)$$

This equation assumes that light is passing from a medium (01) with an index of refraction n_{01} into a medium (12) with an index of refraction n_{12} (Figure 5). The reflection $r(v_i)$ is the usual unpolarized Fresnel reflection coefficient. The Kronecker delta makes both matrices diagonal; this ensures that light is specularly reflected at an angle equal to the incidence angle. The square of the ratio of the indices of refraction accounts for the difference in radiance across a mismatched boundary (due to refraction, also known as the n^2 -law of radiance [35]). Finally, the factor of $2v_i$ ensures conformity with our original definition of the reflection function.

All the angles ν are for light inside the slab. As light leaves the slab it will be refracted and therefore the exiting light angles will differ from ν . Some light will be totally internally reflected and therefore such angles in the slab do not correspond to any physical angle outside the slab. By using interior angles, it is possible to (1) select angles that would otherwise be impossible due to refraction, (2) let the reflection and transmission matrices for the boundaries be diagonal, and (3) optimize the selection of quadrature angles for multiple light scattering. In a air-glass-slab configuration, the critical angle is defined as that for light travelling from a material with index of refraction of the slab to the outside—the presence of a glass slide does affect the maximum angle that light can exit the slab.

The reflection and transmission operators for light travelling from the medium (12) into the medium (01) are

$$\begin{aligned}\mathbf{R}^{10}(\nu_i, \nu_j) &= \mathbf{R}^{01}(\nu_i, \nu_j) \\ \mathbf{T}^{10}(\nu_i, \nu_j) &= \mathbf{T}^{01}(\nu_i, \nu_j) \left(\frac{n_{01}}{n_{12}} \right)^4\end{aligned}\quad (5.58)$$

Since light is refracted at the boundary, care must be taken to ensure that the incident and reflected fluxes are identified with the proper angles. If a glass slide is present at the boundary, then either two separate boundary layers must be added, or a single boundary layer that includes all the multiple internal reflection properties in the glass slide must be used.

If equal boundary conditions exist on both sides of the slab then, by symmetry, the transmission and reflection operator for light travelling from the top to the bottom are equal to those for light propagating from the bottom to the top. Consequently only one set need be calculated. Let the top boundary be layer (01), the turbid slab layer (12), and the bottom layer (23). Since the boundary conditions on each side are equal, we have $\mathbf{R}^{01} = \mathbf{R}^{32}$, $\mathbf{R}^{10} = \mathbf{R}^{23}$, $\mathbf{T}^{01} = \mathbf{T}^{32}$, and $\mathbf{T}^{10} = \mathbf{T}^{23}$. The unusual numbering arises because light exits the medium at the top surface by going from 1 to 0, and leaves through the bottom by going from 2 to 3. The reflection and transmission for the entire slab including boundaries is

$$\mathbf{T}^{03} = \mathbf{T}^{10}(\mathbf{E} - \mathbf{R}^{20}\mathbf{R}^{10})^{-1}\mathbf{T}^{02}\quad (5.59)$$

and

$$\mathbf{R}^{30} = \mathbf{T}^{10}(\mathbf{E} - \mathbf{R}^{20}\mathbf{R}^{10})^{-1}\mathbf{R}^{20}\mathbf{T}^{01} + \mathbf{R}^{01}\quad (5.60)$$

where

$$\mathbf{T}^{02} = \mathbf{T}^{12}(\mathbf{E} - \mathbf{R}^{10}\mathbf{R}^{12})^{-1}\mathbf{T}^{01}\quad (5.61)$$

and

$$\mathbf{R}^{20} = \mathbf{T}^{12}(\mathbf{E} - \mathbf{R}^{10}\mathbf{R}^{12})^{-1}\mathbf{R}^{10}\mathbf{T}^{21} + \mathbf{R}^{21}\quad (5.62)$$

Further increases in efficiency may be made by exploiting the diagonal nature of the reflection and transmission operators for the boundary layers, since most matrix-matrix multiplications above become vector-matrix multiplications.

5.3.5 Example

In this section we show the intermediate calculations necessary for a turbid sample using four integration points. The sample has a single scattering albedo of ($a = 0.9$) and an optical thickness of ($\tau = 1$). The scattering is characterized by Henyey-Greenstein scattering with an anisotropy of ($g = 0.9$). The index of refraction of the sample is $n = 1.5$, and the index of refraction of the surrounding medium is unity. Light interaction at the boundary is assumed to follow Fresnel reflection for unpolarized light.

The first step is to choose appropriate quadrature angles. In this example, the critical angle for total internal reflection is $\theta_c = 41.8^\circ$, which means $\nu_c = 0.745$. Therefore two quadrature angles between 0 and 0.745 are chosen using Gaussian quadrature and two angles between 0.745 and 1 are chosen using Radau quadrature. The resulting quadrature angles and weights using Equations (5.32)–(5.35) are

$$\nu_i = \begin{bmatrix} \nu_1 \\ \nu_2 \\ \nu_3 \\ \nu_4 \end{bmatrix} = \begin{bmatrix} 0.16 \\ 0.59 \\ 0.83 \\ 1.00 \end{bmatrix}$$

$$w_i = \begin{bmatrix} w_1 \\ w_2 \\ w_3 \\ w_4 \end{bmatrix} = \begin{bmatrix} 0.37 \\ 0.37 \\ 0.19 \\ 0.06 \end{bmatrix} \quad (5.63)$$

Note that these angles are measured inside the slab, consequently the two smaller angles correspond to virtual angles in the surrounding medium. These quadrature angles are only slightly different from angles obtained using only Radau quadrature (Equation 5.8). However, the differences in accuracy are dramatic.

When scattering is specified by the Henyey-Greenstein phase function and the anisotropy is 0.9, then the δ - M method requires that the optical depth τ be replaced by $\tau^* \approx 0.410$. Since $\Delta\tau^*$ must be less than ν_1 , and we want $\Delta\tau \cdot 2^n = 1$ (so that n doubling steps will yield a slab with the desired thickness), we find that the largest value of $\Delta\tau^*$ possible is $\Delta\tau^* = 0.102$. This corresponds to $\Delta\tau = 0.25$ and just two doubling steps are needed to reach $\tau = 1$. The redistribution function is found using Equation (5.46)

$$\mathbf{h} = \begin{bmatrix} \mathbf{h}^{--} & \mathbf{h}^{-+} \\ \mathbf{h}^{+-} & \mathbf{h}^{++} \end{bmatrix} \quad (5.64)$$

$$= \begin{bmatrix} \begin{bmatrix} 1.61 & 1.30 & 0.66 & -0.04 \\ 1.30 & 1.94 & 1.96 & 1.74 \\ 0.66 & 1.96 & 3.16 & 4.24 \\ -0.04 & 1.74 & 4.24 & 6.85 \end{bmatrix} & \begin{bmatrix} \mathbf{1.35} & 0.66 & 0.23 & -0.03 \\ \mathbf{0.66} & \mathbf{0.06} & 0.09 & 0.35 \\ \mathbf{0.23} & \mathbf{0.09} & \mathbf{0.12} & 0.15 \\ \mathbf{-0.03} & \mathbf{0.35} & \mathbf{0.15} & \mathbf{-0.37} \end{bmatrix} \\ \begin{bmatrix} 1.35 & 0.66 & 0.23 & -0.03 \\ 0.66 & 0.06 & 0.09 & 0.35 \\ 0.23 & 0.09 & 0.12 & 0.15 \\ -0.03 & 0.35 & 0.15 & -0.37 \end{bmatrix} & \begin{bmatrix} \mathbf{1.61} & \mathbf{1.30} & \mathbf{0.66} & \mathbf{-0.04} \\ 1.30 & \mathbf{1.94} & \mathbf{1.96} & \mathbf{1.74} \\ 0.66 & 1.96 & \mathbf{3.16} & \mathbf{4.24} \\ -0.04 & 1.74 & 4.24 & \mathbf{6.85} \end{bmatrix} \end{bmatrix}$$

Note that the bold face entries are the only unique values because of symmetry e.g., $h(-v_i, -v_j) = h(v_i, v_j)$ and $h(v_i, v_j) = h(v_j, v_i)$.

The reflection and transmission for the starting layer was found using diamond initialization. The reflection and transmission matrices for the initial layer ($\Delta\tau = 0.25$) are

$$\mathbf{R} = \begin{bmatrix} 0.69 & 0.11 & 0.03 & -0.00 \\ 0.11 & 0.01 & 0.00 & 0.01 \\ 0.03 & 0.00 & 0.00 & 0.00 \\ -0.00 & 0.01 & 0.00 & -0.01 \end{bmatrix} \quad (5.65)$$

and

$$\mathbf{T} = \begin{bmatrix} 5.14 & 0.21 & 0.08 & 0.00 \\ 0.21 & 2.02 & 0.07 & 0.05 \\ 0.08 & 0.07 & 2.87 & 0.09 \\ 0.00 & 0.05 & 0.09 & 7.21 \end{bmatrix} \quad (5.66)$$

The negative entries in the reflectance matrix are the result of using a small number of quadrature angles to simulate highly anisotropic scattering. Despite the impossibility of negative reflectances, the integrated quantities R_c and R_d are always positive. If the reflectance at a particular angle for light incident at a particular angle is of interest, then many more quadrature points must be used. This ensures that the highly anisotropic phase functions are approximated accurately. The transmission values on the diagonal of the matrix are much greater than one because unscattered light is included. To include the unscattered light, it must be divided by a factor of $2w_i v_i$ to ensure that the definitions for the integrated quantities, e.g., T_c and T_d are correct.

After doubling the layer thickness once, we have the reflection and transmission for a layer ($\tau = 0.5$) thick,

$$\mathbf{R} = \begin{bmatrix} 0.95 & 0.19 & 0.06 & 0.00 \\ 0.19 & 0.02 & 0.01 & 0.02 \\ 0.06 & 0.01 & 0.01 & 0.01 \\ 0.00 & 0.02 & 0.01 & -0.01 \end{bmatrix} \quad (5.67)$$

and

$$\mathbf{T} = \begin{bmatrix} 3.15 & 0.32 & 0.13 & 0.01 \\ 0.32 & 1.79 & 0.13 & 0.10 \\ 0.13 & 0.13 & 2.61 & 0.17 \\ 0.01 & 0.10 & 0.17 & 6.63 \end{bmatrix} \quad (5.68)$$

Doubling once more yields matrices for a sample with the desired optical thickness $\tau = 1$,

$$\mathbf{R} = \begin{bmatrix} 1.11 & 0.26 & 0.09 & 0.01 \\ 0.26 & 0.04 & 0.02 & 0.03 \\ 0.09 & 0.02 & 0.02 & 0.01 \\ 0.01 & 0.03 & 0.01 & -0.02 \end{bmatrix} \quad (5.69)$$

and

$$\mathbf{T} = \begin{bmatrix} 1.24 & 0.39 & 0.18 & 0.03 \\ 0.39 & 1.43 & 0.22 & 0.17 \\ 0.18 & 0.22 & 2.18 & 0.29 \\ 0.03 & 0.17 & 0.29 & 5.60 \end{bmatrix} \quad (5.70)$$

The layers needed to account for internal reflection at the boundaries are found using the usual unpolarized Fresnel reflection formula

$$\mathbf{R} = \begin{bmatrix} 0.117 & 0 & 0 & 0 \\ 0 & 0.438 & 0 & 0 \\ 0 & 0 & 0.024 & 0 \\ 0 & 0 & 0 & 0.005 \end{bmatrix} \quad (5.71)$$

and

$$\mathbf{T} = \begin{bmatrix} 0.000 & 0 & 0 & 0 \\ 0 & 0.000 & 0 & 0 \\ 0 & 0 & 0.293 & 0 \\ 0 & 0 & 0 & 0.122 \end{bmatrix} \quad (5.72)$$

Adding these boundary layers to the top and bottom of the $\tau = 1$ matrices yields the transport matrices for the entire layer

$$\mathbf{R} = \begin{bmatrix} 8.52 & 0.00 & 0.00 & 0.00 \\ 0.00 & 2.28 & 0.00 & 0.00 \\ 0.00 & 0.00 & 0.41 & 0.07 \\ 0.00 & 0.00 & 0.07 & 0.48 \end{bmatrix} \quad (5.73)$$

and

$$\mathbf{T} = \begin{bmatrix} 0.00 & 0.00 & 0.00 & 0.00 \\ 0.00 & 0.00 & 0.00 & 0.00 \\ 0.00 & 0.00 & 1.92 & 0.29 \\ 0.00 & 0.00 & 0.29 & 5.19 \end{bmatrix} \quad (5.74)$$

Many of the entries are zero because of total internal reflection inside the slab. The total reflection for normal irradiance R_c is found using Equation (5.13). When values from (5.63) and (5.73) into this equation yields

$$R_c = 2(0.83)(0.19)(0.07) + 2(1.00)(0.06)(0.48) = 0.08396 \quad (5.75)$$

Similarly the total transmission for normal irradiance is

$$T_c = 2(0.83)(0.19)(0.29) + 2(1.00)(0.06)(5.19) = 0.75391 \quad (5.76)$$

The discrepancy between the final result and multiplying the terms out is the result of including only two decimal places.

5.4 Calculations

This section gives tables of accurate four digit reflection and transmission results for various albedos and optical thicknesses. The first four tables are calculations for slabs with matched boundary conditions. The last two tables give reflection and transmission values for an air-glass-tissue-glass-air sandwich.

Tables 1 and 2 give reflection and transmission for collimated light normally incident on slabs of various optical depths and albedos. Isotropic scattering was assumed for these tables. Values for reflection and transmission for various optical depths $\tau = 2^{-5}$ to $\tau = 2^5$ and $\tau = \infty$ are identical to those tabulated by van de Hulst [17].

Tables 3 and 4 give reflection and transmission for anisotropic scattering with a Henyey-Greenstein phase function. Many values in this table are identical to those tabulated by van de Hulst ($\tau = 2^0$ to $\tau = 2^4$ and $\tau = \infty$) [36].

The implementation of boundary conditions is verified by comparison with Giovanelli [37] who calculated reflection from a isotropically scattering semi-infinite slab bounded by glass slides. The indices of refraction were $n_{\text{slab}} = 1.333$, $n_{\text{glass}} = 1.532$, and $n_{\text{outside}} = 1.0$. Giovanelli obtains $R_c = 0.6541$ for $a = 0.99$ and the adding-doubling method yields $R_c = 0.6541$. This is satisfactory since Giovanelli states that the fourth digit in his values is questionable. It is unfortunate that more tabulated values for mismatched boundaries are not available in the literature.

Tables 5 and 6 give reflection and transmission for a air-glass-tissue-glass-air sandwich. These values have not been tabulated elsewhere, and may serve as reference values for testing Monte Carlo implementations and various approximate models (e.g., diffusion).

5.5 Conclusions

The adding-doubling method has been implemented with boundary conditions and scattering functions similar to those for many biological tissues. The intermediate details have been described for a sample calculation. The fast and accurate nature of this method for any ratio of scattering to absorption, for any scattering anisotropy, and for any boundary conditions make it useful for all one-dimensional light transport problems. The tabulated of reflection and transmission may be used to evaluate the accuracy of other light transport models.

Total Reflection Matched Boundaries								
n	$a = 1$	$a = .99$	$a = .95$	$a = .9$	$a = .8$	$a = .6$	$a = .4$	$a = .2$
-15	.0000	.0000	.0000	.0000	.0000	.0000	.0000	.0000
-14	.0000	.0000	.0000	.0000	.0000	.0000	.0000	.0000
-13	.0001	.0001	.0001	.0001	.0000	.0000	.0000	.0000
-12	.0001	.0001	.0001	.0001	.0001	.0001	.0000	.0000
-11	.0002	.0002	.0002	.0002	.0002	.0001	.0001	.0000
-10	.0005	.0005	.0005	.0004	.0004	.0003	.0002	.0001
-9	.0010	.0010	.0009	.0009	.0008	.0006	.0004	.0002
-8	.0019	.0019	.0019	.0018	.0016	.0012	.0008	.0004
-7	.0039	.0039	.0037	.0035	.0031	.0023	.0015	.0008
-6	.0078	.0077	.0074	.0069	.0062	.0046	.0030	.0015
-5	.0154	.0152	.0146	.0137	.0121	.0090	.0059	.0029
-4	.0303	.0300	.0286	.0269	.0236	.0173	.0112	.0055
-3	.0589	.0582	.0553	.0518	.0450	.0323	.0207	.0099
-2	.1117	.1101	.1039	.0965	.0824	.0573	.0356	.0167
-1	.2025	.1989	.1851	.1690	.1401	.0927	.0553	.0250
0	.3413	.3329	.3017	.2674	.2108	.1295	.0734	.0320
1	.5175	.4975	.4287	.3616	.2659	.1510	.0820	.0349
2	.6909	.6450	.5124	.4081	.2840	.1553	.0833	.0352
3	.8218	.7288	.5344	.4148	.2853	.1554	.0834	.0352
4	.9036	.7513	.5355	.4149	.2853	.1554	.0834	.0352
5	.9498	.7527	.5355	.4149	.2853	.1554	.0834	.0352
6	.9743	.7527	.5355	.4149	.2853	.1554	.0834	.0352
7	.9870	.7527	.5355	.4149	.2853	.1554	.0834	.0352
8	.9935	.7527	.5355	.4149	.2853	.1554	.0834	.0352
9	.9967	.7527	.5355	.4149	.2853	.1554	.0834	.0352

Table 1: Total reflection from a slab for normal irradiance as a function of optical depth ($\tau = 2^n$) and albedo (a). Scattering is isotropic and the boundary conditions are matched.

Total Transmission Matched Boundaries								
n	$a = 1$	$a = .99$	$a = .95$	$a = .9$	$a = .8$	$a = .6$	$a = .4$	$a = .2$
-15	1.0000	1.0000	1.0000	1.0000	1.0000	1.0000	1.0000	1.0000
-14	1.0000	1.0000	1.0000	1.0000	1.0000	1.0000	.9999	.9999
-13	.9999	.9999	.9999	.9999	.9999	.9999	.9999	.9999
-12	.9999	.9999	.9999	.9999	.9999	.9998	.9998	.9998
-11	.9998	.9998	.9997	.9997	.9997	.9997	.9996	.9996
-10	.9995	.9995	.9995	.9995	.9994	.9993	.9992	.9991
-9	.9990	.9990	.9990	.9989	.9988	.9986	.9984	.9982
-8	.9981	.9980	.9980	.9979	.9977	.9973	.9969	.9965
-7	.9961	.9961	.9959	.9957	.9953	.9945	.9938	.9930
-6	.9922	.9922	.9918	.9914	.9906	.9891	.9875	.9860
-5	.9846	.9844	.9838	.9830	.9814	.9782	.9751	.9721
-4	.9697	.9693	.9680	.9663	.9630	.9567	.9506	.9449
-3	.9411	.9403	.9375	.9340	.9272	.9146	.9030	.8924
-2	.8883	.8867	.8806	.8733	.8595	.8348	.8136	.7951
-1	.7975	.7941	.7808	.7654	.7378	.6928	.6577	.6296
0	.6587	.6510	.6226	.5916	.5414	.4714	.4251	.3923
1	.4825	.4657	.4093	.3565	.2859	.2111	.1730	.1502
2	.3091	.2755	.1869	.1285	.0751	.0394	.0272	.0215
3	.1782	.1221	.0408	.0160	.0046	.0012	.0006	.0004
4	.0964	.0296	.0020	.0002	.0000	.0000	.0000	.0000
5	.0502	.0019	.0000	.0000	.0000	.0000	.0000	.0000
6	.0257	.0000	.0000	.0000	.0000	.0000	.0000	.0000
7	.0130	.0000	.0000	.0000	.0000	.0000	.0000	.0000
8	.0065	.0000	.0000	.0000	.0000	.0000	.0000	.0000
9	.0033	.0000	.0000	.0000	.0000	.0000	.0000	.0000

Table 2: Total transmission by a slab for normal irradiance as a function of optical depth ($\tau = 2^n$) and albedo (a). Scattering is isotropic ($g = 0$) and the boundary conditions are matched.

Total Reflection Matched Boundaries									
n	$g = 0$			$g = .5$			$g = .875$		
	$a = .6$	$a = .9$	$a = .99$	$a = .6$	$a = .9$	$a = .99$	$a = .6$	$a = .9$	$a = .99$
-15	.0000	.0000	.0000	.0000	.0000	.0000	.0000	.0000	.0000
-14	.0000	.0000	.0000	.0000	.0000	.0000	.0000	.0000	.0000
-13	.0000	.0001	.0001	.0000	.0000	.0000	.0000	.0000	.0000
-12	.0001	.0001	.0001	.0000	.0000	.0000	.0000	.0000	.0000
-11	.0001	.0002	.0002	.0000	.0001	.0001	.0000	.0000	.0000
-10	.0003	.0004	.0005	.0001	.0002	.0002	.0000	.0000	.0000
-9	.0006	.0009	.0010	.0002	.0003	.0003	.0000	.0001	.0001
-8	.0012	.0018	.0019	.0004	.0006	.0007	.0001	.0001	.0001
-7	.0023	.0035	.0039	.0008	.0012	.0013	.0001	.0002	.0002
-6	.0046	.0069	.0077	.0016	.0024	.0028	.0003	.0004	.0005
-5	.0090	.0137	.0152	.0031	.0048	.0053	.0005	.0008	.0009
-4	.0173	.0269	.0300	.0060	.0096	.0107	.0010	.0016	.0018
-3	.0323	.0518	.0582	.0114	.0190	.0216	.0019	.0033	.0037
-2	.0573	.0965	.1101	.0208	.0375	.0438	.0035	.0064	.0076
-1	.0927	.1690	.1989	.0352	.0720	.0879	.0059	.0125	.0157
0	.1295	.2674	.3329	.0528	.1298	.1707	.0089	.0238	.0327
1	.1510	.3616	.4975	.0658	.2045	.3053	.0116	.0422	.0691
2	.1553	.4081	.6450	.0698	.2612	.4698	.0128	.0657	.1417
3	.1554	.4148	.7288	.0700	.2770	.6001	.0129	.0826	.2584
4	.1554	.4149	.7513	.0700	.2778	.6561	.0129	.0864	.3753
5	.1554	.4149	.7527	.0700	.2778	.6644	.0129	.0866	.4311
6	.1554	.4149	.7527	.0700	.2778	.6646	.0129	.0866	.4395
7	.1554	.4149	.7527	.0700	.2778	.6646	.0129	.0866	.4397
8	.1554	.4149	.7527	.0700	.2778	.6646	.0129	.0866	.4397
9	.1554	.4149	.7527	.0700	.2778	.6646	.0129	.0866	.4397

Table 3: Total reflection for normal irradiance as a function of optical depth ($\tau = 2^n$) and albedo (a) for three different anisotropies ($g = 0$, $g = 0.5$ and $g = 0.875$) using a Henyey-Greenstein phase function and matched boundary conditions.

Total Transmission Matched Boundaries									
n	$g = 0$			$g = .5$			$g = .875$		
	$a = .6$	$a = .9$	$a = .99$	$a = .6$	$a = .9$	$a = .99$	$a = .6$	$a = .9$	$a = .99$
-15	1.0000	1.0000	1.0000	1.0000	1.0000	1.0000	1.0000	1.0000	1.0000
-14	1.0000	1.0000	1.0000	1.0000	1.0000	1.0000	1.0000	1.0000	1.0000
-13	.9999	.9999	.9999	.9999	1.0000	1.0000	.9999	1.0000	1.0000
-12	.9998	.9999	.9999	.9999	.9999	1.0000	.9999	1.0000	1.0000
-11	.9997	.9997	.9998	.9998	.9999	.9999	.9998	.9999	1.0000
-10	.9993	.9995	.9995	.9995	.9998	.9998	.9996	.9999	1.0000
-9	.9986	.9989	.9990	.9990	.9995	.9996	.9992	.9998	.9999
-8	.9973	.9979	.9980	.9980	.9990	.9993	.9984	.9995	.9998
-7	.9945	.9957	.9961	.9961	.9980	.9986	.9967	.9990	.9997
-6	.9891	.9914	.9922	.9921	.9960	.9972	.9935	.9980	.9994
-5	.9782	.9830	.9844	.9843	.9920	.9944	.9870	.9960	.9988
-4	.9567	.9663	.9693	.9685	.9839	.9886	.9741	.9921	.9975
-3	.9146	.9340	.9403	.9372	.9675	.9770	.9487	.9841	.9950
-2	.8348	.8733	.8867	.8758	.9341	.9533	.8993	.9679	.9898
-1	.6928	.7654	.7940	.7602	.8672	.9057	.8068	.9354	.9790
0	.4714	.5916	.6510	.5629	.7391	.8145	.6458	.8702	.9558
1	.2111	.3565	.4657	.2955	.5233	.6603	.4067	.7432	.9057
2	.0394	.1285	.2755	.0744	.2505	.4527	.1539	.5212	.8001
3	.0012	.0160	.1221	.0041	.0544	.2438	.0197	.2335	.6081
4	.0000	.0002	.0296	.0000	.0025	.0860	.0003	.0410	.3521
5	.0000	.0000	.0019	.0000	.0000	.0120	.0000	.0012	.1263
6	.0000	.0000	.0000	.0000	.0000	.0002	.0000	.0000	.0171
7	.0000	.0000	.0000	.0000	.0000	.0000	.0000	.0000	.0003
8	.0000	.0000	.0000	.0000	.0000	.0000	.0000	.0000	.0000
9	.0000	.0000	.0000	.0000	.0000	.0000	.0000	.0000	.0000

Table 4: Total transmission for normal irradiance as a function of optical depth ($\tau = 2^n$) and albedo (a) for three different anisotropies ($g = 0$, $g = .5$ and $g = 0.875$) using a Henyey-Greenstein phase function and matched boundary conditions.

Total Reflection Glass Boundaries									
n	$g = 0$			$g = .5$			$g = .875$		
	$a = .6$	$a = .9$	$a = .99$	$a = .6$	$a = .9$	$a = .99$	$a = .6$	$a = .9$	$a = .99$
-15	.0789	.0790	.0790	.0789	.0790	.0790	.0789	.0789	.0789
-14	.0790	.0790	.0790	.0789	.0790	.0790	.0789	.0789	.0790
-13	.0790	.0790	.0790	.0789	.0790	.0790	.0789	.0789	.0790
-12	.0790	.0790	.0790	.0790	.0790	.0790	.0789	.0790	.0790
-11	.0790	.0791	.0791	.0790	.0790	.0791	.0789	.0790	.0790
-10	.0790	.0792	.0793	.0790	.0791	.0792	.0789	.0790	.0790
-9	.0791	.0795	.0797	.0790	.0792	.0794	.0789	.0790	.0790
-8	.0793	.0801	.0805	.0790	.0795	.0799	.0789	.0790	.0791
-7	.0796	.0812	.0821	.0790	.0801	.0808	.0788	.0791	.0793
-6	.0801	.0834	.0853	.0791	.0812	.0825	.0786	.0792	.0797
-5	.0813	.0878	.0915	.0793	.0834	.0861	.0782	.0795	.0804
-4	.0835	.0962	.1037	.0795	.0877	.0932	.0774	.0800	.0819
-3	.0875	.1120	.1269	.0800	.0959	.1069	.0760	.0809	.0850
-2	.0939	.1399	.1695	.0804	.1107	.1331	.0732	.0827	.0910
-1	.1025	.1831	.2408	.0801	.1348	.1801	.0682	.0857	.1029
0	.1098	.2348	.3429	.0775	.1659	.2547	.0606	.0902	.1263
1	.1123	.2721	.4569	.0724	.1883	.3482	.0518	.0944	.1693
2	.1122	.2835	.5540	.0693	.1905	.4339	.0464	.0920	.2328
3	.1122	.2845	.6134	.0691	.1886	.4973	.0454	.0823	.2875
4	.1122	.2845	.6307	.0691	.1885	.5273	.0454	.0786	.3096
5	.1122	.2845	.6319	.0691	.1885	.5320	.0454	.0784	.3165
6	.1122	.2845	.6319	.0691	.1885	.5321	.0454	.0784	.3176
7	.1122	.2845	.6319	.0691	.1885	.5321	.0454	.0784	.3176
8	.1122	.2845	.6319	.0691	.1885	.5321	.0454	.0784	.3176
9	.1122	.2845	.6319	.0691	.1885	.5321	.0454	.0784	.3176

Table 5: Total reflection as a function of optical depth ($\tau = 2^n$) and albedo (a) for three different anisotropies ($g = 0$, $g = .5$, and $g = 0.875$) using a Henyey-Greenstein phase function. The slab ($n_{\text{slab}} = 1.4$) is bounded by glass ($n_{\text{glass}} = 1.5$) and air ($n_{\text{air}} = 1.0$).

Total Transmission Glass Boundaries									
n	$g = 0$			$g = .5$			$g = .875$		
	$a = .6$	$a = .9$	$a = .99$	$a = .6$	$a = .9$	$a = .99$	$a = .6$	$a = .9$	$a = .99$
-15	.9210	.9210	.9210	.9210	.9210	.9210	.9210	.9210	.9211
-14	.9210	.9210	.9210	.9210	.9210	.9210	.9210	.9210	.9210
-13	.9210	.9210	.9210	.9210	.9210	.9210	.9210	.9210	.9210
-12	.9209	.9209	.9209	.9209	.9210	.9210	.9209	.9210	.9210
-11	.9207	.9208	.9208	.9207	.9209	.9209	.9208	.9210	.9210
-10	.9203	.9205	.9206	.9204	.9207	.9208	.9206	.9209	.9210
-9	.9195	.9200	.9202	.9198	.9203	.9205	.9202	.9207	.9209
-8	.9180	.9189	.9193	.9186	.9196	.9200	.9194	.9204	.9208
-7	.9151	.9167	.9176	.9162	.9181	.9190	.9177	.9198	.9205
-6	.9091	.9123	.9142	.9114	.9151	.9170	.9144	.9185	.9200
-5	.8973	.9037	.9075	.9018	.9092	.9130	.9077	.9159	.9189
-4	.8741	.8868	.8942	.8829	.8975	.9050	.8946	.9107	.9168
-3	.8294	.8540	.8689	.8462	.8745	.8893	.8688	.9003	.9125
-2	.7465	.7925	.8220	.7768	.8299	.8592	.8191	.8796	.9038
-1	.6043	.6842	.7417	.6535	.7468	.8040	.7275	.8386	.8861
0	.3952	.5149	.6210	.4605	.6046	.7116	.5718	.7590	.8501
1	.1682	.2988	.4696	.2266	.3999	.5812	.3495	.6139	.7786
2	.0299	.1038	.3042	.0535	.1805	.4252	.1266	.3918	.6521
3	.0009	.0127	.1447	.0028	.0382	.2504	.0154	.1568	.4770
4	.0000	.0002	.0358	.0000	.0017	.0924	.0002	.0259	.2823
5	.0000	.0000	.0023	.0000	.0000	.0130	.0000	.0007	.1039
6	.0000	.0000	.0000	.0000	.0000	.0003	.0000	.0000	.0142
7	.0000	.0000	.0000	.0000	.0000	.0000	.0000	.0000	.0003
8	.0000	.0000	.0000	.0000	.0000	.0000	.0000	.0000	.0000
9	.0000	.0000	.0000	.0000	.0000	.0000	.0000	.0000	.0000

Table 6: Total transmission as a function of optical depth ($\tau = 2^n$) and albedo (a) for three different anisotropies ($g = 0.0, g = 0.5$ and $g = 0.875$) using a Henyey-Greenstein phase function. The slab ($n_{\text{slab}} = 1.4$) is bounded by glass ($n_{\text{glass}} = 1.5$) and air ($n_{\text{air}} = 1$).

References

- [1] S. A. Prahl, M. J. C. van Gemert, and A. J. Welch, "Determining the optical properties of turbid media by using the adding-doubling method," *Appl. Opt.*, vol. 32, pp. 559–568, 1993.
- [2] J. W. Pickering, S. A. Prahl, N. van Wieringen, J. F. Beek, H. J. C. M. Sterenborg, and M. J. C. van Gemert, "Double-integrating-sphere system for measuring the optical properties of tissue," *Appl. Opt.*, vol. 32, pp. 399–410, 1993.
- [3] J. A. Parrish, "New concepts in therapeutic photomedicine: Photochemistry, optical targeting and the therapeutic window," *J. Invest. Dermatol.*, vol. 77, pp. 44–50, 1981.
- [4] W. F. Cheong, S. A. Prahl, and A. J. Welch, "A review of the optical properties of biological tissues," *IEEE J. Quantum Electron.*, vol. 26, pp. 2166–2185, 1990.
- [5] S. L. Jacques, C. A. Alter, and S. A. Prahl, "Angular dependence of HeNe laser light scattering by human dermis," *Lasers Life Sci.*, vol. 1, pp. 309–333, 1987.
- [6] A. Ishimaru, *Wave Propagation and Scattering in Random Media*, vol. 1. New York: Academic Press, 1978.
- [7] K. M. Case and P. F. Zweifel, *Linear Transport Theory*. Reading: Addison-Wesley Publishing Co., 1967.
- [8] B. C. Wilson and G. Adam, "A Monte Carlo model for the absorption and flux distributions of light in tissue," *Med. Phys.*, vol. 10, pp. 824–830, 1983. monte carlo.
- [9] S. A. Prahl, M. Keijzer, S. L. Jacques, and A. J. Welch, "A Monte Carlo model of light propagation in tissue," in *SPIE Proceedings of Dosimetry of Laser Radiation in Medicine and Biology* (G. J. Müller and D. H. Sliney, eds.), vol. IS 5, pp. 102–111, 1989. monte carlo.
- [10] M. Keijzer, S. L. Jacques, S. A. Prahl, and A. J. Welch, "Light distributions in artery tissue: Monte Carlo simulations for finite-diameter laser beams," *Lasers Surg. Med.*, vol. 9, pp. 148–154, 1989. monte carlo.
- [11] L. Reynolds, C. C. Johnson, and A. Ishimaru, "Diffuse reflectance from a finite blood medium: Applications to the modeling of fiber optic catheters," *Appl. Opt.*, vol. 15, pp. 2059–2067, 1976.
- [12] R. F. Bonner, R. Nossal, S. Havlin, and G. H. Weiss, "Model for photon migration in turbid biological media," *J. Opt. Soc. Am. A*, vol. 4, pp. 423–432, 1987.
- [13] P. Kubelka, "New contributions to the optics of intensely light-scattering materials. Part I," *J. Opt. Soc. Am.*, vol. 38, pp. 448–457, 1948.
- [14] G. Yoon, S. A. Prahl, and A. J. Welch, "Accuracies of the diffusion approximation and its similarity relations for laser irradiated biological media," *Appl. Opt.*, vol. 28, pp. 2250–2255, 1989.
- [15] S. Chandrasekhar, *Radiative Transfer*. New York: Dover, 1960.
- [16] K. N. Liou, "A numerical experiment on Chandrasekhar's discrete ordinate method for radiative transfer: Applications to cloudy and hazy atmospheres," *J. Atmos. Sci.*, vol. 30, pp. 1303–1326, 1973.
- [17] H. C. van de Hulst, *Multiple Light Scattering*, vol. 1. New York: Academic Press, 1980.
- [18] G. N. Plass, G. W. Kattawar, and F. E. Catchings, "Matrix operator theory of radiative transfer. 1: Rayleigh scattering," *Appl. Opt.*, vol. 12, pp. 314–329, 1973.
- [19] H. C. van de Hulst, "A new look at multiple scattering," tech. rep., NASA Institute for Space Studies, New York, 1962.
- [20] W. M. Irvine, "Multiple scattering in planetary atmospheres," *Icarus*, vol. 25, pp. 175–204, 1975.

- [21] I. P. Grant and G. E. Hunt, “Discrete space theory of radiative transfer I. Fundamentals,” *Proceedings of the Royal Society of London A*, vol. A313, pp. 183–197, 1969.
- [22] I. P. Grant and G. E. Hunt, “Discrete space theory of radiative transfer II. Stability and non-negativity,” *Proceedings of the Royal Society of London A*, vol. A313, pp. 199–216, 1969.
- [23] J. E. Hansen and L. D. Travis, “Light scattering in planetary atmospheres,” *Space Science Reviews*, vol. 16, pp. 525–610, 1974.
- [24] W. J. Wiscombe, “On initialization, error and flux conservation in the doubling method,” *J. Quant. Spectrosc. Radiat. Transfer*, vol. 16, pp. 637–658, 1976.
- [25] S. A. Prahl, *Light Transport in Tissue*. PhD thesis, University of Texas at Austin, 1988.
- [26] H. H. Michels, “Abscissas and weight coefficients for Lobatto quadrature,” *Mathematical Computation*, vol. 17, pp. 237–244, 1963.
- [27] F. B. Hildebrand, *Introduction to Numerical Analysis*. New York: Dover Publications, 1974.
- [28] W. H. Press, B. P. Flannery, S. A. Teukolsky, and W. T. Vetterling, *Numerical Recipes: The Art of Scientific Computing*. New York: Cambridge University Press, 1986.
- [29] H. C. van de Hulst and M. M. Davis *Proc. Koninkl. Nederl. Akad. Wet.*, vol. B64, p. 220, 1961.
- [30] W. J. Wiscombe, “The range of validity of the Eddington approximation,” *Icarus*, vol. 32, pp. 362–377, 1977.
- [31] J. H. Joseph, W. J. Wiscombe, and J. A. Weinman, “The delta-Eddington approximation for radiative flux transfer,” *J. Atmos. Sci.*, vol. 33, pp. 2452–2459, 1976.
- [32] I. P. Grant and G. E. Hunt, “Solution of radiative transfer problems using the invariant S_n method,” *Monthly Notices of the Royal Astronomical Society*, vol. 141, pp. 27–41, 1968.
- [33] W. M. Irvine, “Multiple scattering by large particles,” *Astrophys. J.*, vol. 142, pp. 1463–1475, 1965.
- [34] W. J. Wiscombe, “Doubling initialization revisited,” *J. Quant. Spectrosc. Radiat. Transfer*, vol. 18, pp. 245–248, 1977.
- [35] R. W. Preisendorfer, *Hydrologic Optics*. U. S. Department of Commerce, 1976.
- [36] H. C. van de Hulst, *Multiple Light Scattering*, vol. 2. New York: Academic Press, 1980.
- [37] R. G. Giovanelli, “Reflection by semi-infinite diffusers,” *Optica Acta*, vol. 2, pp. 153–162, 1955.